A STUDY OF NUMERICAL METHODS FOR COMPUTING REENTRY TRAJECTORIES FOR SHUTTLE-TYPE SPACE VEHICLES

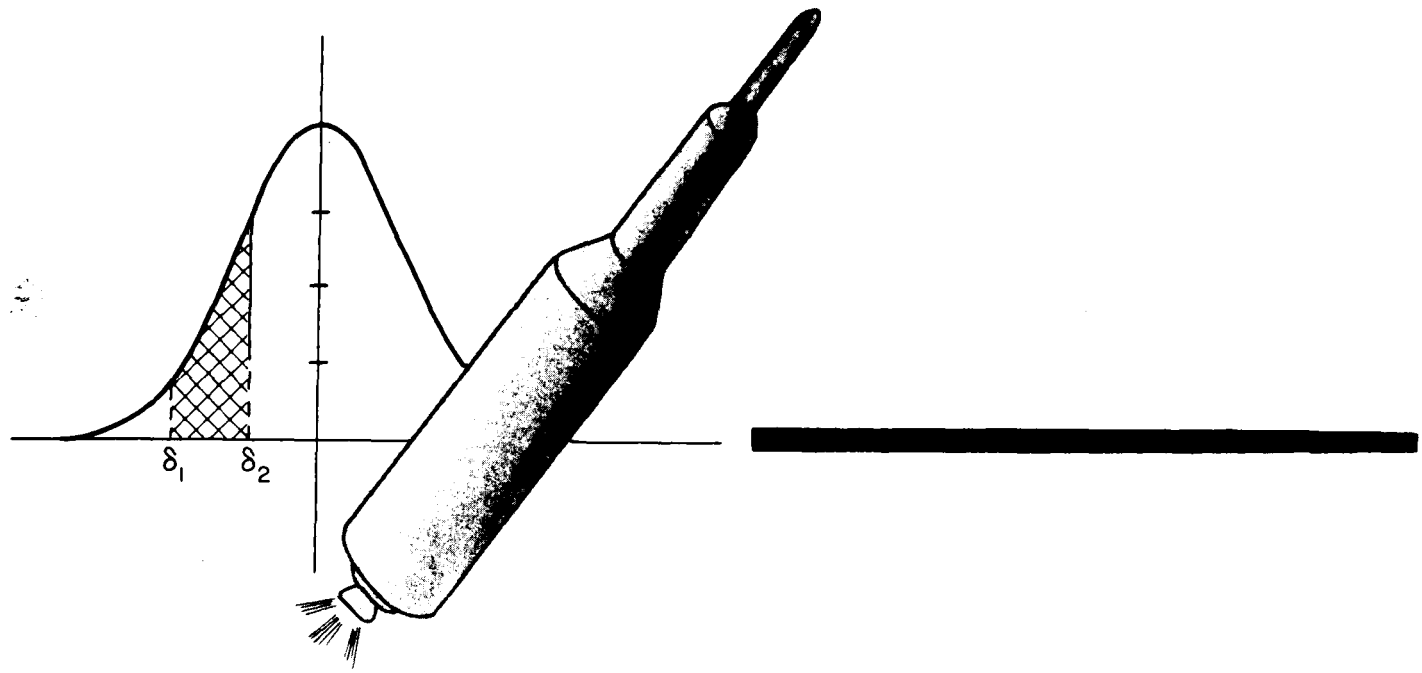

TEXAS CENTER FOR RESEARCH
3100 PERRY LANE, AUSTIN, TEXAS

Final Report for Contract NAS 9-11964, Mod. 1S

A STUDY OF NUMERICAL METHODS FOR COMPUTING REENTRY TRAJECTORIES FOR SHUTTLE-TYPE SPACE VEHICLES

Prepared for

National Aeronautics and Space Administration

Manned Spacecraft Center

Houston, Texas

by

Texas Center for Research

Applied Mathematics and Mechanics

3100 Perry Lane

Austin, Texas 78731

TABLE OF CONTENTS

LIST OF FIGURES

List of Symbols

The following is a list of all symbols used in this study, accompanied by a brief description. Vectors are indicated by brackets with the dimensions of the variable in the brackets. Matrices are denoted by brackets with both dimensions given within the brackets.

$A[2n \times 2n]$	Matrix of partial derivatives of F with respect to z (i.e., $\frac{\partial F}{\partial z}$)
A_w	Constant associated with the linear function relating insulation weight per unit area to total heat load per unit area.
$a[6]$	Coefficients of polynomial representing transition region for the boundary layer function g.
B_w	Constant associated with the linear function relating insulation weight per unit area to total heat load per unit area.
$b[n_p]$	Coefficients used in the definition of y.
$C[q]$	Control variable inequality constraints
C_D	Aerodynamic drag coefficient
C_{D_L}	Constant associated with Newtonian flow drag equation
C_{D_o}	Drag coefficient at zero angle of attack
C_L	Aerodynamic lift coefficient
C_{L_o}	Constant associated with Newtonian flow lift equation
$c[n_p]$	Coefficients used in the definition of y.
D	Aerodynamic drag
E	Lift: drag ratio
e_r	Unit vector in the direction of increasing r.
e_θ	Unit vector in the direction of increasing θ.

e_ϕ	Unit vector in the direction of increasing ϕ .
e_{x_w}	Unit vector in the direction of v .
e_{x_b}	Unit vector along the zero lift line of the vehicle.
e_{y_w}	Unit vector directed out the left side of the vehicle forming a righthand system with e_{x_w} and e_{z_w} .
e_{z_w}	Unit vector lying in the plane of symmetry of the vehicle.
e_{z_b}	Unit vector lying in the plane of symmetry of the vehicle forming a right-hand system with e_{x_b} and e_{y_b} .
F[2n]	The derivatives with respect to time states and multipliers evaluated using the optimal control.
f[n]	The derivatives with respect to time of the state variables.
$g[n_p]$	Boundary layer function relating the effects of the nature of the flow within the boundary layer to the heating rate.
H	Variational Hamiltonian
h[n + 1]	Boundary conditions for optimization problem
I[n x n]	Identity matrix
J	Performance index
k	Gravitational constant for the earth
k_c	Convective heat transfer constant
k_d	Density constant
k_g	Boundary layer function constant
k_R	Reynolds number constant
L	Aerodynamic lift
ℓ	Number of control variables
M[p]	Terminal constraints
m	Mass of vehicle
n	Number of state variables

n_p	Number of panels comprising the thermal protection system
p	Number of terminal constraints
Q	Integrand of performance index
$\dot{Q}_c$	Convective heating rate
q	Number of control variable inequality constraints
$\dot{q}_o$	Reference heating rate, at the stagnation point on a one-foot radius sphere
$R_L[n_p]$	Reynolds number per foot at which transition from laminar to turbulent flow begins on a panel.
R_n	Reference Reynolds number per foot
r	Radial distance from the center of the earth to the reentry vehicle.
r_e	Radius of the earth
S	Vehicle reference area
S_*	Vehicle reference area per unit mass
$s[n_p]$	Panel areas
$T[n_p]$	Panel temperatures
t	Independent variable, time
t_o	Initial time
t_f	Final time
$u[\ell]$	Control variables
V	Velocity magnitude
V_c	Circular orbital speed at $r = r_e$.
W	Weight of the vehicle
W_{TPS}	Weight of the thermal protection system
$w[n_p]$	Weight of the insulation on a panel
$x[n]$	State variables
$y[n_p]$	Functions which account for the effect of angle of attack
$z[2n]$	Variables consisting of states and multipliers
α	Angle of attack

β	Roll angle
γ	Flight path angle
ε_s	Surface emissivity
$\zeta[3]$	Parameter used in defining the partial derivatives of the optimal angle of attack
η	Angle used in defining the optimal angle of attack
θ	Longitude
$\lambda[n]$	Lagrange multipliers associated with the states
λ_c	Weighting factor
$\mu[q]$	Lagrange multipliers associated with the control variable inequality constraints
ρ	Atmospheric density
ρ_o	Atmospheric density at the surface of the earth
σ	Stephan-Boltzman constant
$\Phi[2n \times 2n]$	Fundamental matrix
$\Phi_1[2n \times 2n]$	First n columns of the fundamental matrix
$\Phi_2[2n \times 2n]$	Last n columns of the fundamental matrix
ϕ	Latitude
ψ	Heading angle

Special Symbols

$\delta( )$	Variation of ( ) holding t constant
$\Delta( )$	Total variation in ( )
$\dot{( )}$	Derivative with respect to t
$( )^T$	Transpose
$(\cdot)^{-1}$	Inverse
$\frac{d}{dt}( )$	Derivative of ( ) with respect to t
$\frac{\partial}{\partial t}( )$	Partial derivative of ( ) with respect to t
$( )_x$	Partial derivative of ( ) with respect to x

Abbreviations

MPF	Method of Perturbation Functions
TPBVP	Two-Point Boundary Value Problem
TPS	Thermal Protection System
REI	Reuseable External Insulation
CVIC	Control Variable Inequality Constraint

I. Introduction

The design procedure for any complex system is typically one of compromise and trade-off. The design of the space shuttle reentry vehicle is certainly no exception because numerous factors demand attention and contribute to the performance capability of the vehicle.

A primary consideration in the design of any reentry vehicle is the aerodynamic heating which the vehicle will encounter upon reentry. The total heat input and the associated temperatures directly determine the amount of thermal protection necessary for the safe reentry of the vehicle. The amount of thermal protection required is particularly important because the resultant weight is usually a significant portion of the vehicle weight. Consequently, weight penalties incurred by excessive heating reduce the payload capability with a resultant increase in payload delivery cost. Therefore, trajectories which yield minimal weight penalties due to heating effects are desirable in order to improve the operational efficiency of the vehicle.

Of the suggested models for the Thermal Protection System (TPS), the Reuseable Exterior Insulation system (REI) is the model selected for this study. The REI system is composed of titanium covered by a surface insulation material. The insulation is used on that portion of the surface where the local temperature exceeds 650° F. Additional internal insulation is utilized on all fuselage and wing areas which exceed 650° F.

To estimate the weight of the TPS, the surface of the vehicle is divided into n panels. The weight of each panel is related to the total heat transferred to the panel during reentry. A typical variation of exterior insulation weight per unit surface area with heat load is indicated in Figure 1.

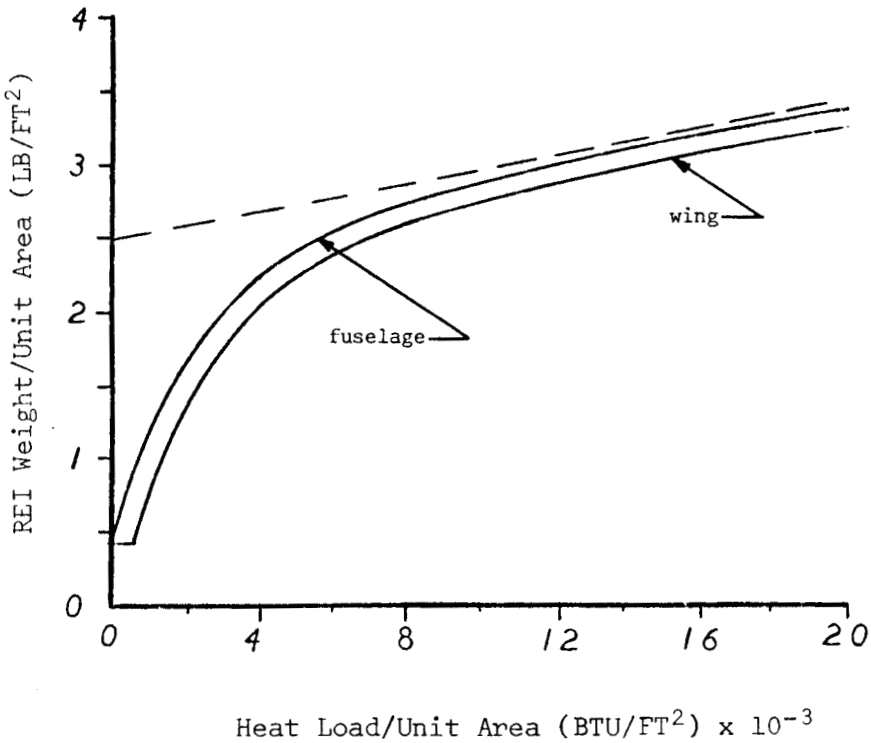

Figure 1. REI Weight Versus Heat Load

If the curves shown above are approximated by a linear function as indicated by the dashed line, the TPS weight can be related to the heat load to the n panels as follows:

$$W_{TPS} = \sum_{i=1}^{n} w_i \tag{1.1}$$

where

$$w_i = A_w + B_w Q_i \tag{1.2}$$

or

$$W_{TPS} = \sum_{i=1}^{n} (A_w + B_w Q_i) \tag{1.3}$$

A_w and B_w are constants while Q_i is the heat load to the i-th panel. Consequently, with these simplifications the TPS weight is linearly related to the heat load, and the minimization of the TPS weight is analogous to minimization of the total heat load.

II. Performance Index

In the present study only the four lower-surface panels of the fuselage are considered. In addition, for reentry velocities on the order of earth orbital speed, aerodynamic heating is composed primarily of convective heating.[1] Therefore, the heating rate to the underside of the fuselage is represented by the sum of the convective heating rates to the four individual panels, and the performance index to be minimized is the integrated heat input to these panels.

$$J = \lambda_c \int_{t_o}^{t_f} \dot{Q}_c dt \tag{2.1}$$

where λ_c is a constant scale factor and $\dot{Q}_c$ is the convective heating rate to the selected panels, given by

$$\dot{Q}_c = \dot{q}_o \sum_{i=1}^{4} s_i y_i g_i \tag{2.2}$$

The reference heating rate, $\dot{q}_o$, is the heating rate which would occur at the stagnation point on a one-foot radius sphere following the same path as the vehicle, that is,

$$\dot{q}_o = k_c \rho^{0.5} V^{3.15} \tag{2.3}$$

where k_c is a constant, ρ is the atmospheric density and V is the magnitude of the velocity. The area of the i-th panel is designated by s_i. The function g_i is a boundary layer dependent function which relates the effects of the nature of the flow in the boundary layer on the heating rate to the i-th panel. It is defined[5] to be the following second-derivative-continuous function:

$$g_i = 1, \quad \frac{R_n}{R_{L_i}} \leq 1.0 \quad \text{(Laminar)}$$

$$g_i = \sum_{j=0}^{5} a_{j+1} \left(\frac{R_n}{R_{L_i}}\right)^j, \quad 1.0 \leq \frac{R_n}{R_{L_i}} \leq 1.5 \quad \text{(Transition)} \qquad (2.4)$$

$$g_i = k_g \left(\frac{R_n}{R_{L_i}}\right)^{0.3}, \quad \frac{R_n}{R_{L_i}} \geq 1.5 \quad \text{(Turbulent)}$$

where R_n is the reference Reynolds number per foot

$$R_n = k_R \left(\frac{\rho V^2}{\dot{q}_o 1/2}\right)^{1.5} \qquad (2.5)$$

In these formulas, k_g, k_R, a_j are constants and R_{L_i} is the boundary layer transition Reynolds number for the i-th panel. The function y_i is introduced to account for the effect of angle of attack on the heating rate to the i-th panel. The particular form of y_i was chosen because it expresses the expected influence of α and was simple to implement. The expression for y_i is given as

$$y_i(\alpha) = b_i + c_i |\sin^3\alpha| \qquad (2.6)$$

where b_i and c_i are constants determined by fitting y_i to experimental data and α is the angle of attack.

III. Dynamical Model

The dynamical model for the atmospheric reentry is chosen to be as uncomplicated as practical and yet retain the salient characteristics of a more exact formulation. In particular, the earth is assumed to be spherical, non-rotating and to possess an inverse square gravitational force field. The atmosphere is considered to be at rest with respect to the earth and to vary exponentially with altitude.

The spacecraft is located relative to the earth via a spherical coordinate system whose origin is fixed at the center of the earth as illustrated in Figure 2. The distance from the center of the earth to the vehicle is designated by r, while the longitude and latitude of the vehicle are represented by θ and ϕ, respectively.

The velocity vector, with magnitude V, is oriented in space by using the heading angle, ψ, and the flight path angle, γ as indicated in Figure 3. The attitude of the vehicle is then established by a roll angle, β, about the velocity vector followed by an angle of attack, α, about the vehicle's lateral axis as shown in Figure 4. Zero sideslip angle is assumed.

In this system, the equations governing the motion of the vehicle are[3]

$$\begin{aligned}
\dot{r} &= V \sin \gamma \\
\dot{\theta} &= \frac{V \cos \gamma \cos \psi}{r \cos \phi} \\
\dot{\phi} &= \frac{V \cos \gamma \sin \psi}{r} \\
\dot{V} &= -\frac{k \sin \gamma}{r^2} - \frac{D}{m} \\
\dot{\gamma} &= -\frac{k \cos \gamma}{Vr^2} \bullet \frac{V \cos \gamma}{r} + \frac{L}{mV} \cos \beta \\
\dot{\psi} &= -\frac{V \cos \gamma \cos \psi \tan \phi}{r} - \frac{L \sin \beta}{mV \cos \gamma}
\end{aligned} \tag{3.1}$$

where k is the gravitational constant of the earth, m is the mass of the vehicle, L is the lift of the vehicle, D is the drag of the vehicle and motion of the vehicle about its center of mass is ignored. Lift and drag are defined in the conventional manner as

$$\begin{aligned}
L &= (1/2)\ \rho V^2 S C_L \\
\text{and} \qquad D &= (1/2)\ \rho V^2 S C_D
\end{aligned} \tag{3.2}$$

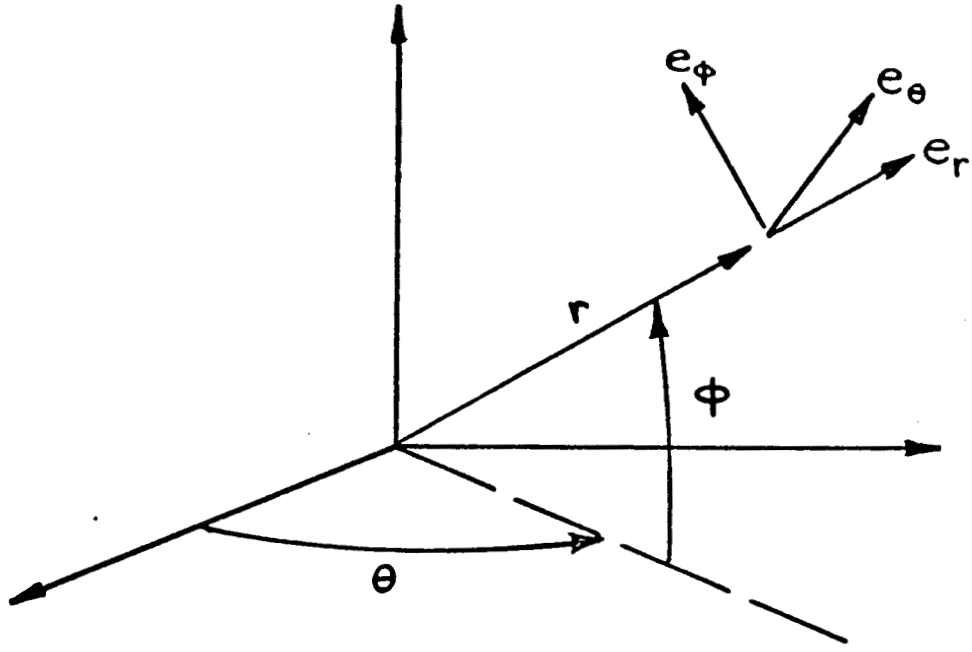

Figure 2. Earth-Centered Coordinate System

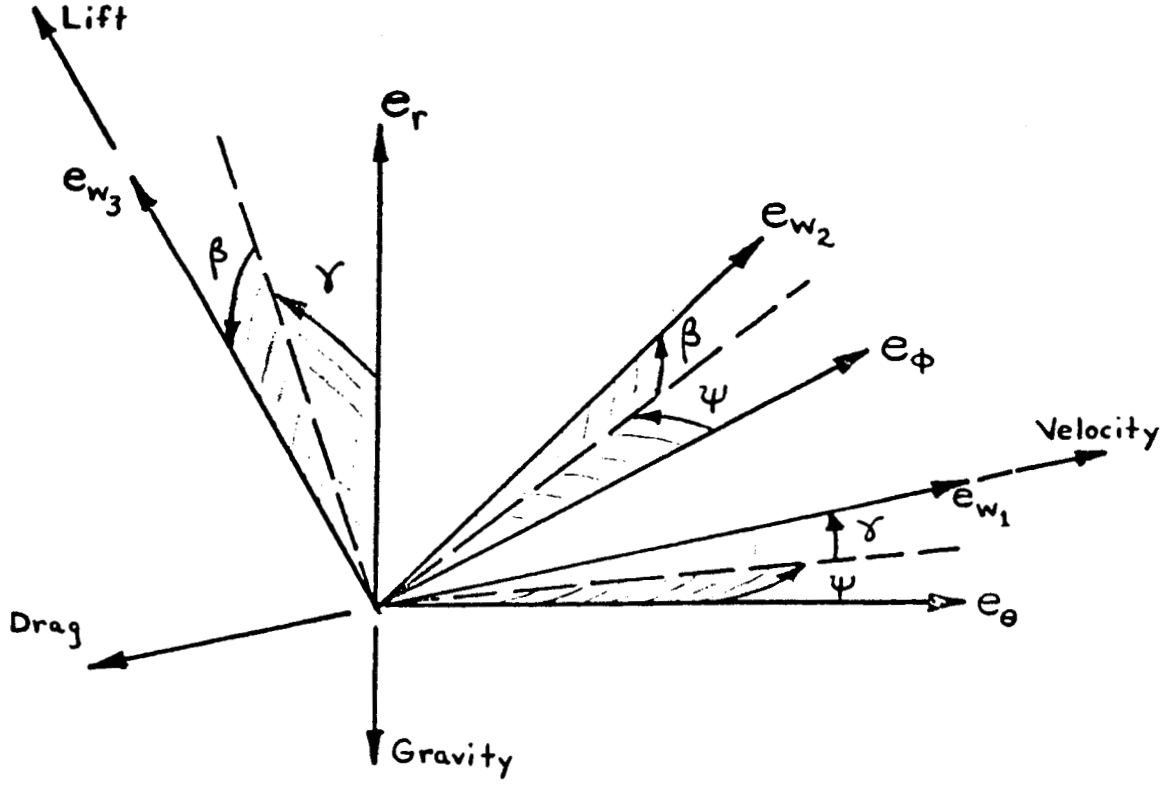

Figure 3. Body-Centered Wind Axis System

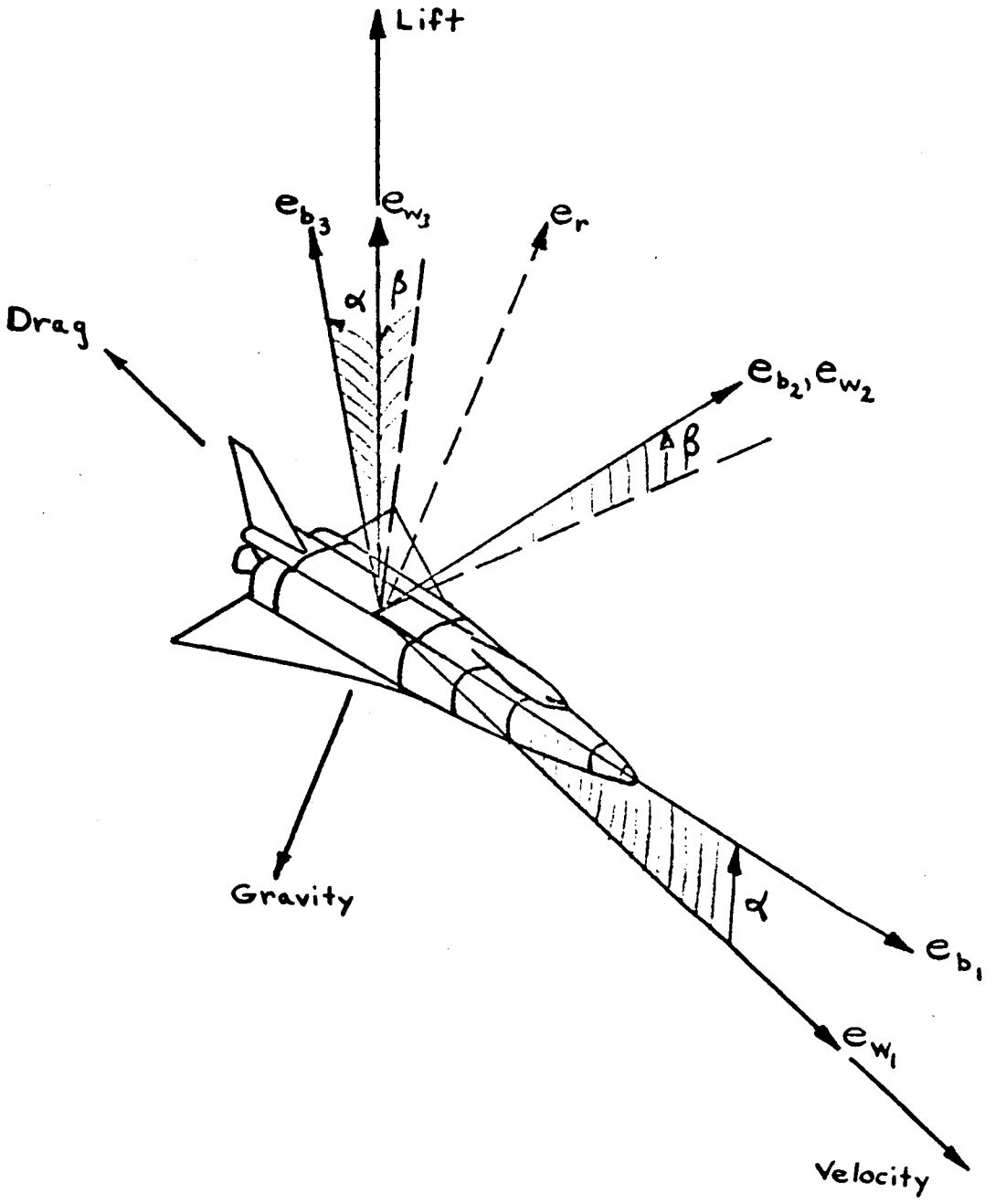

Figure 4. Definition of Control Angles

where S is the vehicle reference area and C_L and C_D are coefficients of lift and drag, respectively. The atmospheric density, ρ, is assumed to vary exponentially with altitude according to

$$\rho = \rho_o{}^{-k_d(r-r_e)} \tag{3.3}$$

where ρ_o and k_d are constants chosen[3] to approximate the density of the actual atmosphere over the altitudes of interest for reentry and where r_e is the radius of the earth.

The aerodynamic coefficients C_L and C_D are generally functions of the Mach number and of the Reynolds number as well as the angle of attack. However, for hypersonic flight, the drag coefficient is essentially independent of the Mach number and for high altitude flight the effects of Reynolds number are relatively unimportant in comparison with those due to angle of attack. Consequently, the lift and drag coefficients are assumed to be functions of angle of attack only and are given by the following relationships[8,9] obtained from Newtonian flow theory:

$$C_L = C_{L_o} \sin \alpha \cos \alpha \, |\sin \alpha| \tag{3.4}$$

$$C_D = C_{D_o} + C_{D_L} \, |\sin^3 \alpha| \tag{3.5}$$

where C_{L_o}, C_{D_o} and C_{D_L} are constants. The lift-to-drag ratio, E, is then given as

$$E = \frac{C_{L_o} \sin \alpha \cos \alpha \, |\sin \alpha|}{C_{D_o} + C_{D_L} \sin^3 \alpha |} \tag{3.6}$$

The dependence of C_L, C_D and E upon angle of attack for the vehicle of this study is illustrated in Figure 5.

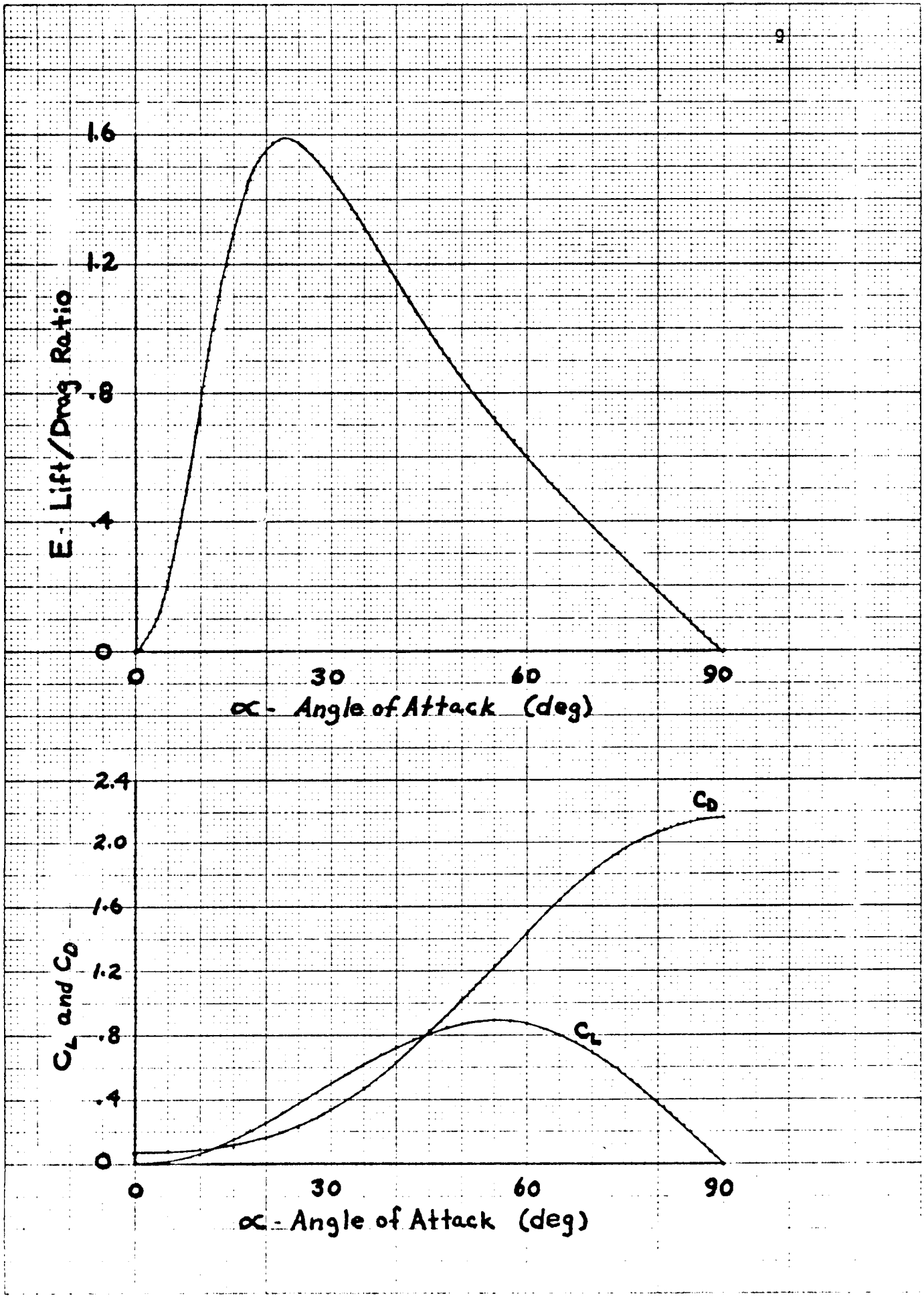

Figure 5. Aerodynamic Coefficients versus Angle of Attack

IV. Control Variable Inequality Constraints

The reentry vehicle is controlled by varying the angle of attack, α, which determines the magnitude of the aerodynamic force and the roll angle, β, which determines the direction of the lift force. Although for the analysis of this study, β is not necessarily subject to physical limitation, α must certainly be limited. The desire to reduce heating on the upper surface of the vehicle requires that α be non-negative. In addition, the obvious constraint that α not exceed 90 degrees must be imposed. However, more exact modeling requires even closer restrictions to be placed on the angle of attack. For example, control power and stability boundaries for a typical configuration place additional constraints upon the angle of attack as illustrated in Figure 6.[12]

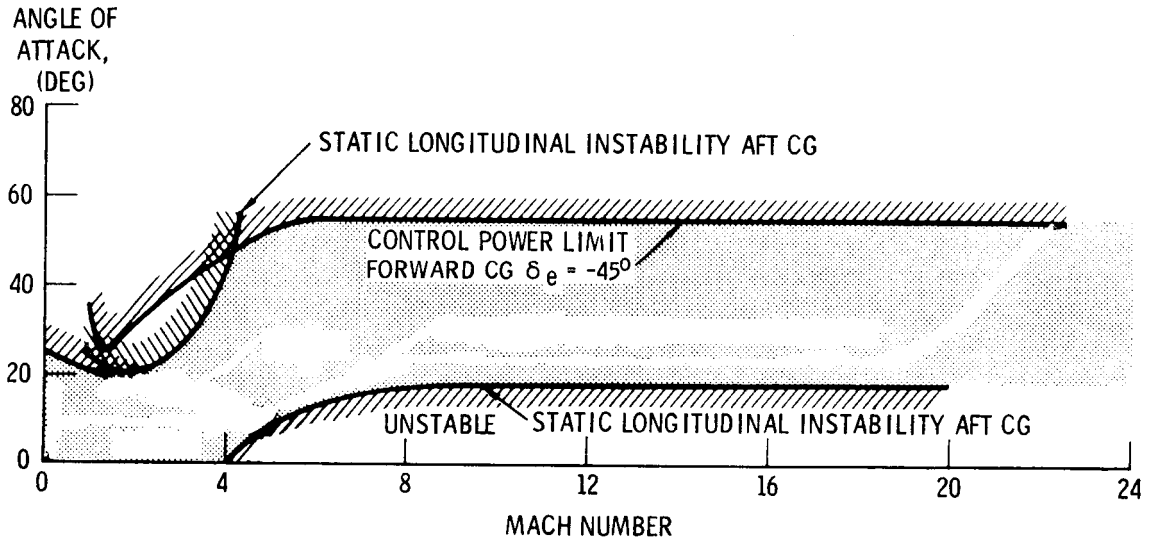

Figure 6. Angle of Attack Boundaries versus Mach Number

In accordance with such restrictions, the angle of attack limits are chosen to be

$$\alpha_{max} = 55°$$
$$\alpha_{min} = 15° \qquad (4.1)$$

Note that the maximum angle of attack is approximately equal to the angle of attack for maximum lift coefficient.

Minimization of heat load is usually accomplished by producing high peak heating rates over short time intervals. This is done by flying a trajectory which is composed of a sequence of skip segments in which the vehicle dives down into the atmosphere until sufficient lift is generated to force it back up into the thinner atmosphere. For a vehicle constrained to positive angles of attack, the skip is produced by first rolling down ($|\beta| \geq 90°$) . This produces a downward component of lift which forces the vehicle down into the atmosphere. The pull-up is then accomplished by rolling up. Skipping maneuvers such as these can produce high peak altitudes as well as high heating rates requiring increased accuracy from the guidance system. As a means of reducing the adverse effects of the skipping phenomenon, a maximum roll angle is implemented to reduce the vehicle's ability to dive into the atmosphere. Therefore, the constraints applied to the roll angle are

$$\beta_{max} = 70°$$
$$\beta_{min} = 0° \qquad (4.2)$$

V. Boundary Conditions

The immediate projected use of the shuttle vehicle is that of transporting men and equipment to orbiting earth satellites or space laboratories. Therefore, the initial conditions for reentry will remain approximately the same for most of its missions. The nominal values selected for this investigation

are indicated below:

$$
\begin{aligned}
r_o - r_e &= 400{,}000 \text{ ft} \\
\theta_o &= 0 \\
\phi_o &= 0 \\
V_o &= 25{,}975 \text{ ft/sec} \\
\gamma_o &= -1.5 \text{ deg} \\
\psi_o &= 0 \\
t_o &= 0
\end{aligned}
\tag{5.1}
$$

The shuttle vehicle represents, in many respects, a significant departure from previous operational reentry vehicles. The increased hypersonic lift-to-drag ratio (1.5 to 2.0) of the shuttle enables it to achieve a larger reentry footprint. In addition, the utilization of engines for subsonic cruise further increases the footprint size and enables the vehicle to land as a conventional aircraft. Therefore, the amount of crossrange and downrange required for a specific mission quite naturally depends upon orbit inclination, the location of an acceptable landing site, the location of the deorbit maneuver and subsonic range capability. In order to define the reentry optimization problem, tne following nominal terminal conditions are imposed

$$
\begin{aligned}
\theta_f &= 6200 \text{ mi}/r_e \text{ radians} \\
\phi_f &= -1880 \text{ mi}/r_e \text{ radians} \\
V_f &= 3000 \text{ ft/sec}
\end{aligned}
\tag{5.2}
$$

VI. The Perturbation Method

The previous sections define the reentry optimization problem treated in this study to be of the following form:

$$
J = \int_{t_o}^{t_f} Q(x,u,t)dt \tag{6.1}
$$

subject to the differential constraints,

$$\dot{x} = f(x,u,t) \tag{6.2}$$

the control variable inequality constraints,

$$C(x,u,t) \leq 0 \tag{6.3}$$

the initial conditions

$$\begin{aligned} x(t_o) &= x_o \\ t_o &= 0 \end{aligned} \tag{6.4}$$

and the terminal conditions

$$M(x_f,t_f) = 0 \tag{6.5}$$

where Q is a scalar function, x is an n-vector of state variables, u is an ℓ vector of control variables, C is a q vector of control variable constraints, x_o is an n-vector of initial conditions, t_o is the initial time and M is a p vector of terminal conditions.

The necessary conditions[2] for a minimum are written as:

$$\dot{x} = H_\lambda^T(x,u,t) \tag{6.6}$$

$$\dot{\lambda} = - H_x^T(x,u,\lambda,\mu,t) \tag{6.7}$$

$$0 = H_u(x,u,\lambda,\mu,t) \tag{6.8}$$

where λ is an n-vector of time dependent Lagrange multipliers associated with the states and H is the variational Hamiltonian,

$$H = Q + \lambda^T f + \mu^T C \tag{6.9}$$

with

$$\begin{aligned} \mu_i &= 0 \quad \text{when} \quad C_i < 0 \\ \mu_i &> 0 \quad \text{when} \quad C_i = 0 \end{aligned} \tag{6.10}$$

where μ is an ℓ-vector of multipliers associated with the control variable inequality constraints and where the matrix H_{uu} must be positive definite.

The following boundary conditions must be satisfied:

$$x = x_o \quad \text{at} \quad t = t_o \tag{6.11}$$

and

$$\begin{aligned} H(t_f) &= 0 \\ \lambda(t_f) &= \nu^T M_x(x_f, t_f) \quad \text{at} \quad t = t_f \\ M(x_f, t_f) &= 0 \end{aligned} \tag{6.12}$$

where ν is a p-vector of constant multipliers associated with the specified terminal conditions.

Elimination of the control u by using Eqs. (6.8) and (6.10) reduces the optimization problem to a two-point boundary value problem (TPBVP) which is stated in the following way:

Find the unknown elements of z_o and the final time t_f which yield the solution of

$$\dot{z} = F(z,t) \tag{6.13}$$

where

$$z = \begin{bmatrix} x \\ - - \\ \lambda \end{bmatrix} \tag{6.14}$$

and

$$F = \begin{bmatrix} H_\lambda^T \\ - - - - - - \\ - H_x^T \end{bmatrix} \tag{6.15}$$

Such that the $(n+1)$ vector, $h(z_f, t_f)$, of terminal constraints, composed of Eq. (6.12) vanishes.

Numerous techniques are available for solution of two-point boundary value problems. The technique used in this study is the method of perturbation functions (MPF) discussed in Ref. 3 and 7.

To initiate the method, the unknown elements of the vector z_o (in this study the Lagrange multipliers, λ_o) and the final time are selected in some way. A nominal trajectory is then

obtained by integrating Eqs. (6.13) from t_o to t_f. Since this trajectory seldom satisfies the terminal conditions, a correction procedure is required to determine the necessary changes in λ_o and t_f ($\delta\lambda_o$ and δt_f). This is accomplished by considering small perturbations about the nominal path through linearization of the nonlinear differential equations and terminal conditions as follows:

$$\delta\dot{z} = A\delta z \tag{6.16}$$

where

$$A = \left[\frac{\partial F}{\partial z}\right] \qquad (2n \times 2n \text{ matrix}) \tag{6.17}$$

Also, the expected change in the terminal dissatisfaction is written as

$$\Delta h = \left[\frac{\partial h}{\partial z}\right]_f \delta z_f + \left[\dot{h}\right]_f \delta t_f \tag{6.18}$$

where

$$\left[\dot{h}\right]_f = \left[\frac{\partial h}{\partial z}\right]_f \dot{z}_f + \frac{\partial h}{\partial t_f} \tag{6.19}$$

If it is desired to satisfy the end conditions in one iteration, Δh is chosen to be

$$\Delta h = - h \tag{6.20}$$

so that

$$- h = \left[\frac{\partial h}{\partial z}\right]_f \delta z_f + \left[\dot{h}\right]_f \delta t_f \tag{6.21}$$

The changes δz_f are related to the changes δz_o in this linearized system by the fundamental matrix,[4] $\Phi(t_f,t_o)$, according to

$$\delta z_f = \Phi(t_f,t_o)\delta z_o \tag{6.22}$$

where Φ obeys the following linear matrix differential equation and initial condition

$$\dot{\Phi}(t,t_o) = A\Phi(t,t_o) \quad (2n \times 2n \text{ matrix}) \tag{6.23}$$

$$\Phi(t_o,t_o) = \left[\begin{array}{c|c} I & 0 \\ \hline 0 & I \end{array}\right] \tag{6.24}$$

where I is an n x n identity matrix and 0 is an n x n null matrix.

Since all initial states are specified, only the effect of perturbations in the initial multipliers must be computed. Therefore, only the right half or the last n columns of the fundamental matrix must be integrated. Following this idea, let

$$\Phi = \left[\Phi_1 \;\vdots\; \Phi_2\right] \tag{6.25}$$

then

$$\dot{\Phi}_2 = A\Phi_2 \quad (2n \times n \text{ matrix})$$
$$\Phi_2(t_o,t_o) = \left[\begin{array}{c} 0 \\ \hline I \end{array}\right] \tag{6.26}$$

and

$$\delta z_f = \Phi_2(t_f,t_o)\delta\lambda_o \tag{6.27}$$

By using this result, Eq. (6.21) is rewritten as

$$-h = \left[\frac{\partial h}{\partial z}\right]_f \Phi_2(t_f,t_o)\delta\lambda_o + \left[\dot{h}\right]_f \delta t_f \tag{6.28}$$

Solution of this system of n + 1 simultaneous linear equations yields the changes $\delta\lambda_o$ and δt_f which, if the TPBVP were linear, would produce a new vector λ_o and final time t_f capable of satisfying the terminal constraints. However, the nonlinear nature of most optimization problems requires an iterative procedure in which only a portion of the predicted correction is applied on each iterate in an effort to maintain the validity of the linearization process. The technique used in this study for scaling the corrections is the same as that used by Williamson,[3] and Lastman and Tapley[7] in which the scale factor is computed

such that the magnitude of the correction vector never exceeds a prescribed fraction (e.g., 0.30) of the magnitude of the initial vector of multipliers, λ_o .

With the preceding discussion in mind, the basic algorithm of the MPF is presented as follows:

1. Guess nominal starting values for λ_o and t_f .
2. Integrate the differential equations for the states and the multipliers simultaneously with the linear perturbation equations from t_o to t_f .
3. Evaluate the dissatisfaction in the terminal conditions and compute the changes $\delta\lambda_o$ and δt_f .
4. Add the scaled changes to the previous values for λ_o and t_f and repeat steps 2 through 4 until the dissatisfaction in the terminal conditions is considered small.

VII. Numerical Integration

The integration of the differential equations for this investigation was performed using the variable stepsize Runge-Kutta 7(8) formulation developed and described by Fehlberg[6]. A relative single-step truncation error analysis, based on the leading term of the truncation error for the seventh-order formulation in which both the linear and nonlinear equations were considered, was used in computing the stepsize.

The units used in the integration of the differential equations are miles, radians and miles per second. The use of these units affords a form of normalization of the variables and multipliers which tends to aid in the convergence characteristics of the problem. All numerical computation was performed in single precision on the CDC 6600/6400 computer system at the University of Texas at Austin.

VIII. Application of the MPF and Numerical Results

The MPF requires the optimization problem to be reduced to a TPBVP. Therefore, begin by writing the variational Hamiltonian for the reentry as

$$H = Q + \lambda_r V \sin\gamma + \lambda_\theta \frac{V\cos\gamma\cos\psi}{r\cos\phi} + \lambda_\phi \frac{V\cos\gamma\sin\psi}{r}$$
$$+ \lambda_V\left(-\frac{k\sin\gamma}{r^2} - \frac{1}{2}\rho V^2 S_* C_D\right) +$$
$$+ \lambda_\gamma\left(-\frac{k\cos\gamma}{Vr^2} + \frac{V\cos\gamma}{r} + \frac{1}{2}\rho V S_* C_L\cos\beta\right) \qquad (8.1)$$
$$+ \lambda_\psi\left(-\frac{V\cos\gamma\cos\psi\tan\phi}{r} - \frac{1}{2}\rho V S_* C_L\frac{\sin\beta}{\cos\gamma}\right)$$
$$+ \mu_\alpha(\alpha_{max} - \alpha)(\alpha_{min} - \alpha) + \mu_\beta(\beta_{max} - \beta)(\beta_{min} - \beta)$$

where $S_* = \frac{S}{m}$.

The differential equations for the multipliers associated with the states,

$$\dot{\lambda} = -H_x^T \qquad (8.2)$$

then become

$$\dot{\lambda}_r = -Q_r + \lambda_\theta\frac{V\cos\gamma\cos\psi}{r^2\cos\phi} + \lambda_\phi\frac{V\cos\gamma\sin\psi}{r^2}$$
$$- \lambda_V\left(\frac{2k\sin\gamma}{r^3} - \frac{1}{2}\rho_r V^2 S_* C_D\right)$$
$$- \lambda_\gamma\left(\frac{2k\cos\gamma}{Vr^3} - \frac{V\cos\gamma}{r^2} + \frac{1}{2}\rho_r V S_* C_L\cos\beta\right) \qquad (8.3)$$
$$- \lambda_\psi\left(\frac{V\cos\gamma\cos\psi\tan\phi}{r^2} - \frac{1}{2}\rho_r V S_* C_L\frac{\sin\beta}{\cos\gamma}\right)$$

$$\dot{\lambda}_\theta = 0 \qquad (8.4)$$

$$\dot{\lambda}_\phi = -\lambda_\theta\frac{V\cos\gamma\cos\psi\sin\phi}{r\cos^2\phi} + \lambda_\psi\frac{V\cos\gamma\cos\psi}{r\cos^2\phi} \qquad (8.5)$$

$$\dot{\lambda}_V = -Q_V - \lambda_r\sin\gamma - \lambda_\theta\frac{\cos\gamma\cos\psi}{r\cos\phi} - \lambda_\phi\frac{\cos\gamma\sin\psi}{r}$$
$$+ \lambda_V\rho V S_* C_D - \lambda_\gamma\left(\frac{k\cos\gamma}{V^2r^2} + \frac{\cos\gamma}{r} + \frac{1}{2}\rho S_* C_L\cos\beta\right)$$
$$+ \lambda_\psi\left(\frac{\cos\gamma\cos\psi\tan\phi}{r} + \frac{1}{2}\rho S_* C_L\frac{\sin\beta}{\cos\gamma}\right) \qquad (8.6)$$

$$\dot{\lambda}_\gamma = -\lambda_r V\cos\gamma + \lambda_\theta \frac{V\sin\gamma\cos\psi}{r\cos\phi} + \lambda_\phi \frac{V\sin\gamma\sin\psi}{r}$$
$$+ \lambda_V \frac{k\cos\gamma}{r^2} - \lambda_\gamma\left(\frac{k\sin\gamma}{Vr^2} - \frac{V\sin\gamma}{r}\right)$$
$$- \lambda_\psi\left(\frac{V\sin\gamma\cos\psi\tan\phi}{r} - \frac{1}{2}\rho V S_* C_L \frac{\sin\beta\tan\gamma}{\cos\gamma}\right) \qquad (8.7)$$

$$\dot{\lambda}_\psi = \lambda_\theta \frac{V\cos\gamma\sin\psi}{r\cos\phi} - \lambda_\phi \frac{V\cos\gamma\cos\psi}{r} - \lambda_\psi \frac{V\cos\gamma\sin\psi\tan\phi}{r} \qquad (8.8)$$

where

$$Q = \lambda_c \dot{q}_o \sum_{i=1}^{4} s_i g_i y_i \qquad (8.9)$$

$$Q_r = \lambda_c \sum_{i=1}^{4} [(\dot{q}_o g_{r_i} + \dot{q}_{o_r} g_i) s_i y_i] \qquad (8.10)$$

$$Q_V = \lambda_c \sum_{i=1}^{4} [(\dot{q}_o g_{V_i} + \dot{q}_{o_V} g_i) s_i y_i] \qquad (8.11)$$

and

$$\dot{q}_{o_r} = 0.5\, k_c \rho^{-.5} \rho_r V^{3.15} \qquad (8.12)$$

$$\dot{q}_{i_V} = 3.15\, k_c \rho^{.5} V^{2.15} \qquad (8.13)$$

$$\rho_r = -k_d \rho \qquad (8.14)$$

The partial derivatives of the boundary layer function, g_i, are written as

$$g_{x_i} = \frac{\partial g_i}{\partial x} = \frac{\partial g_i}{\partial R_n}\frac{\partial R_n}{\partial x} \qquad (8.15)$$

Since g_i is dependent upon the ratio R_n/R_{L_i}, so are its derivatives.

$$\frac{\partial g_i}{\partial R_n} = 0 \qquad \frac{R_n}{R_{L_i}} \leq 1.0$$

$$\frac{\partial g_i}{\partial R_n} = R_{L_i}^{-1} \sum_{j=1}^{5} j a_{j+1} \left(\frac{R_n}{R_{L_i}}\right)^{j-1} \qquad 1.0 \leq \frac{R_n}{R_{L_i}} \leq 1.5$$

$$\frac{\partial g_i}{\partial R_n} = .3\, k_g R_{L_i}^{-1} \left(\frac{R_n}{R_{L_i}}\right)^{-.7} \qquad \frac{R_n}{R_{L_i}} \geq 1.5 \tag{8.16}$$

In addition,

$$\frac{\partial R_n}{\partial r} = 1.125\, k_R \rho^{.5} \rho_r V^3 \dot{q}_o^{-3/4} \tag{8.17}$$

and

$$\frac{\partial R_n}{\partial V} = 0.6375\, k_R \rho^{3/2} V^2 \dot{q}_o^{-3/4} \tag{8.18}$$

The optimal control is determined by requiring $H_\alpha = 0$, $H_\beta = 0$ and the matrix H_{uu} given by

$$H_{uu} = \left[\begin{array}{c|c} H_{\alpha\alpha} & H_{\alpha\beta} \\ \hline H_{\beta\alpha} & H_{\beta\beta} \end{array}\right]$$

to be positive definite.

From these conditions, the optimal roll angle is given by

$$\sin \beta = \frac{\lambda_\psi}{(\lambda_\psi^2 + \lambda_\gamma^2 \cos^2 \gamma)^{1/2}}$$

$$\cos \beta = \frac{-\lambda_\gamma \cos \gamma}{(\lambda_\psi^2 + \lambda_\gamma^2 \cos^2 \gamma)^{1/2}} \tag{8.19}$$

The optimal angle of attack is given by

$$\alpha = \frac{1}{2}\left[\eta + \arcsin\left(\frac{1}{3}\sin\eta\right)\right] \qquad -\pi \leq \eta \leq \pi \tag{8.20}$$

where

$$\sin\eta = (\lambda_\psi \sin\beta - \lambda_\gamma \cos\gamma \cos\beta)/P$$

$$\cos\eta = \left(\frac{\lambda_c \dot{q}_o}{\frac{1}{2}\rho V S_* C_{L_o}} \sum_{i=1}^{4} s_i g_i c_i - \frac{\lambda_V V C_{D_L}}{C_{L_o}}\right)\cos\gamma/P$$

and

$$P = [\cos^2 \gamma (\frac{\lambda_c \dot{q}_o}{\frac{1}{2}\rho V S_* C_{L_o}} \sum_{i=1}^{4} s_i g_i c_i - \frac{\lambda_V V C_{D_L}}{C_{L_o}}) + (\lambda_\gamma \cos \gamma \cos \beta - \lambda_\psi \sin \beta)^2]^{1/2} \quad (8.21)$$

The boundary conditions for the TPBVP are summarized as follows

$$\text{at } t = t_o$$

$$\begin{aligned} r_o - r_e &= 400{,}000 \text{ feet} \\ \theta_o &= 0 \\ \phi_o &= 0 \\ V_o &= 25{,}975 \text{ feet/second} \\ \gamma_o &= -1.5 \text{ degrees} \\ \psi_o &= 0 \end{aligned} \quad (8.22)$$

$$\text{at } t = t_f$$

$$\begin{aligned} \lambda_{r_f} &= 0 \qquad (r_f \text{ free}) \\ \theta_f &= 6200/r_e \text{ radians} \\ \phi_f &= -1880/r_e \text{ radians} \\ V_f &= 3000 \text{ feet/second} \\ \lambda_{\gamma_f} &= 0 \qquad (\gamma_f \text{ free}) \\ \lambda_{\psi_f} &= 0 \qquad (\psi_f \text{ free}) \\ H_f &= 0 \qquad (t_f \text{ free}) \end{aligned} \quad (8.23)$$

The values for the unknown initial multipliers, λ_o, and the final time, t_f for the trajectory presented are listed below

$$\lambda_{r_o} = -1.54294713 \times 10^{-2}$$

$$\lambda_{\theta_o} = -3.24144967 \times 10^{-4}$$

$$\lambda_{\phi_o} = 3.08551281 \times 10^{-1}$$

$$\lambda_{V_o} = -1.52864923 \times 10^{1}$$

$$\lambda_{\gamma_o} = 1.04803561 \times 10$$

$$\lambda_{\psi_o} = 59.9992066 \times 10$$

$$t_f = 2039.729 \text{ seconds}$$

Graphical representation of the resultant trajectory is presented in Figures 7 through 11.

The optimal angle of attack and roll angle are plotted versus time in Figure 7. Whereas, the maximum roll angle constraint is encountered twice, the angle of attack encounters its minimum boundary only once, near the end of the trajectory. For the major portion of the trajectory the optimal angle of attack is very nearly that for E_{MAX}. This is not unusual because the specified crossrange is near the maximum crossrange for the vehicle and the downrange is considerable, which normally requires high values for E.

The time histories for altitude, velocity and flight path angle are presented in Figure 8; while those for downrange crossrange and heading angle are presented in Figure 9. Referring back to Figure 7, it is seen that the roll angle is at its maximum during the initial reentry phase and the first altitude peak, which supports the contention that a roll angle constraint would reduce skip altitudes. The terminal flight path angle is approximately -22°. Although for operational reasons a value nearer zero might be more desirable, the terminal altitude and velocity should be adequate to allow the necessary transition to powered flight.

The reference heating rate, $\dot{q}_o$, the dynamic pressure and aerodynamic load factor are plotted versus time in Figure 10.

The peak heating rate of 124 BTU/(FT2-SEC) which occurs at the bottom of the first altitude pull-up, is followed by lesser peaks occurring each time the minimum altitude in a pull-up maneuver is reached. Dynamic pressure and load factor reach their maximum values of approximately 266 psf and 1.42 g's, respectively, at the end of the trajectory. The maximum load factor is well within projected limits for space-rated personnel.

The temperatures on the fuselage panels considered in this study (computed from the following equation

$$T_i = \left(\frac{\dot{Q}_i}{\varepsilon_s \sigma}\right)^{1/4} - 460° \qquad (°F) \qquad (8.24)$$

where ε_s is the surface emissivity and σ is the Stephan-Boltzman constant) are plotted versus time in Figure 11.

The maximum temperatures attained are

$$T_{1_{MAX}} = 2249° \text{ F}$$

$$T_{2_{MAX}} = 1649° \text{ F}$$

$$T_{3_{MAX}} = 1509° \text{ F}$$

$$T_{4_{MAX}} = 1607° \text{ F}$$

The effect of the growth of the turbulent boundary layer on the temperatures is evident in the distinct change in character of the heating on panel 4 at approximately $t = 1200$ seconds. The heating to each panel exhibits this effect in turn as the transition point moves toward the front of the vehicle.

The value of the total heat load to which the four panels are subjected for this high crossrange trajectory is computed to be 3.276×10^7 BTU's. As expected, other trajectories with lower crossrange have lower heat loads. In particular, trajectories computed for crossrange on the order of 1700 miles have produced heat loads on the order of 2.5×10^7 BTU's.

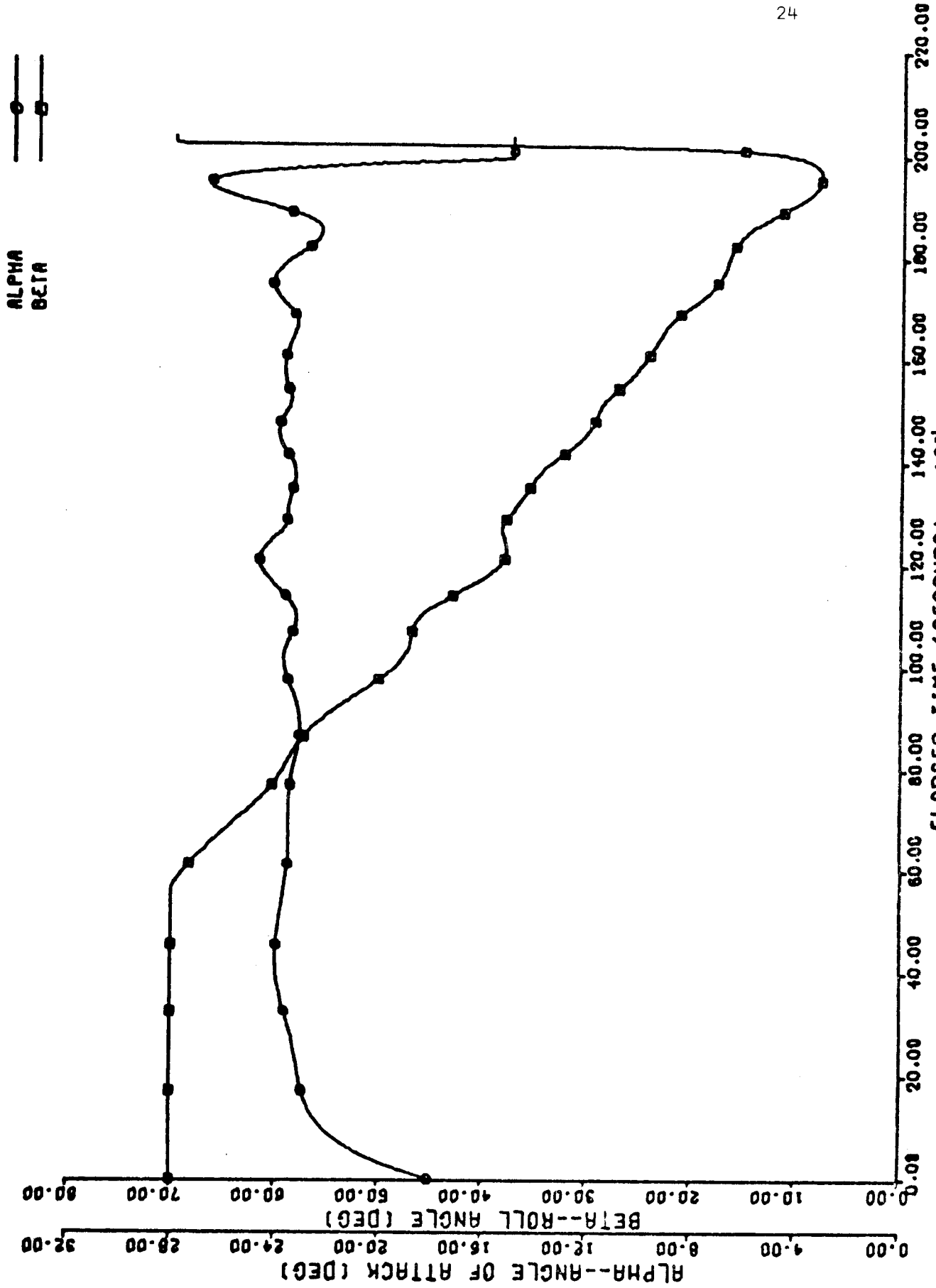

Figure 7. Angle of Attack and Roll Angle versus Time

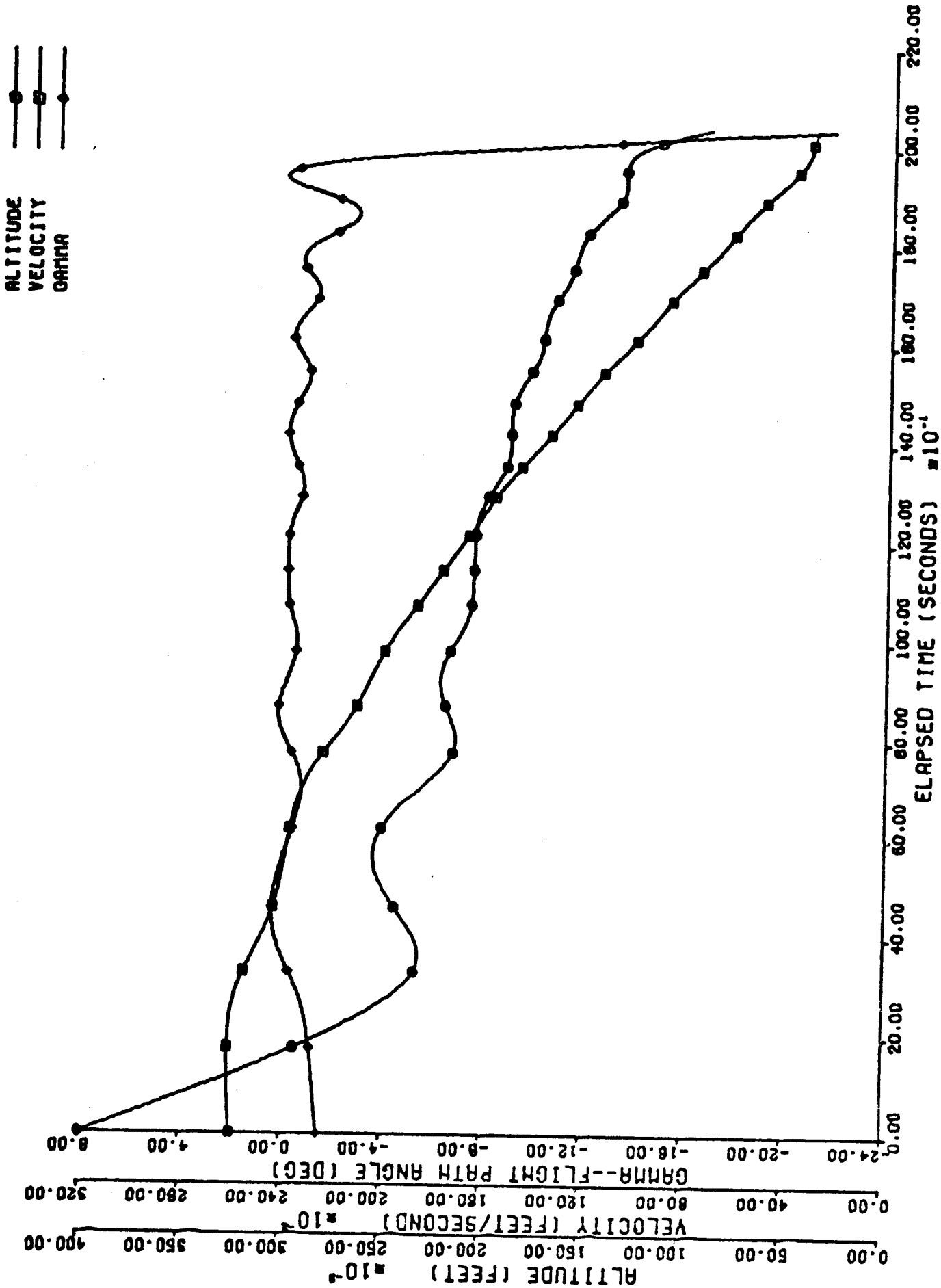

Figure 8. Altitude, Velocity, and Flight Path Angle versus Time

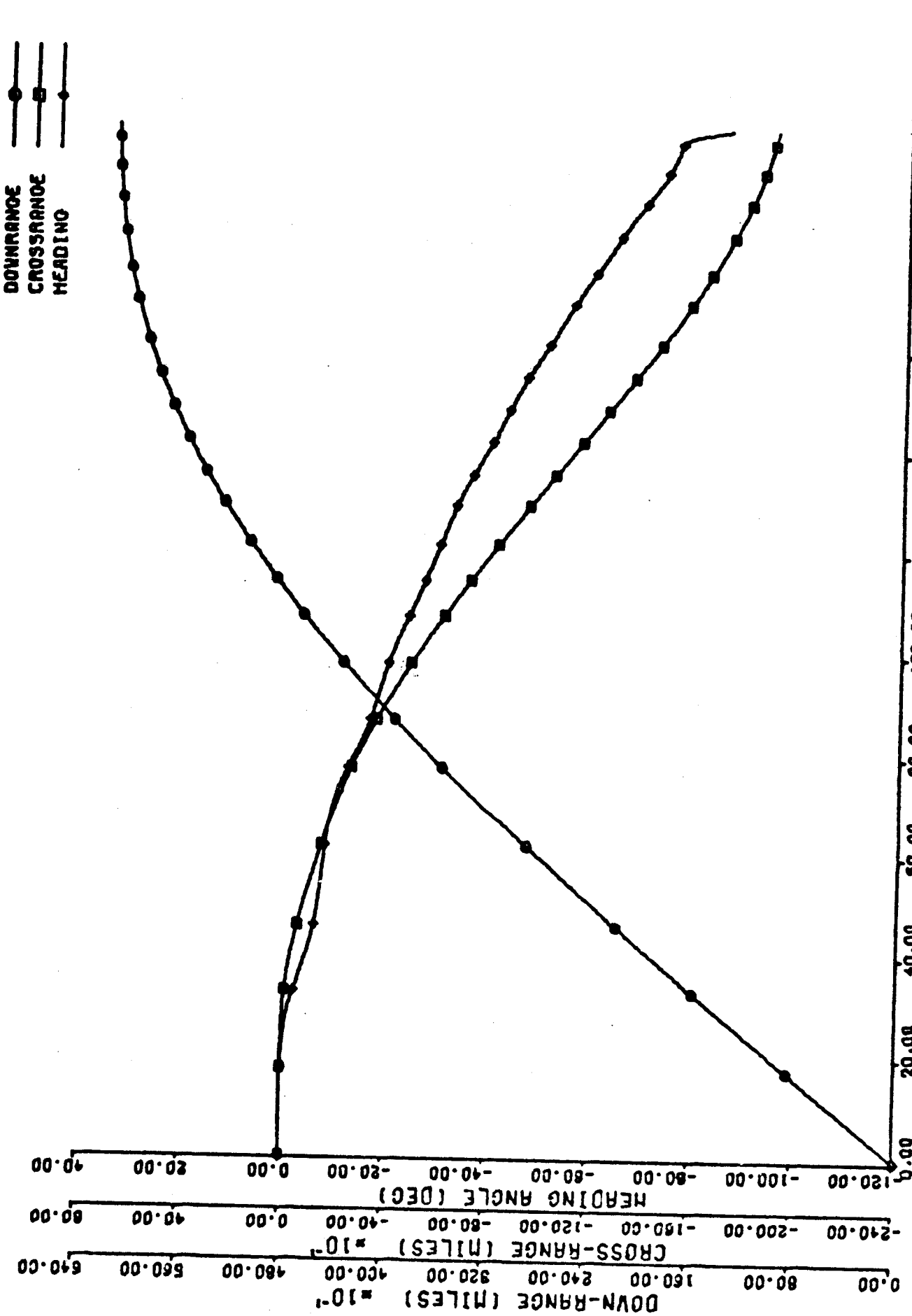

Figure 9. Downrange, Crossrange and Heading Angle versus Time

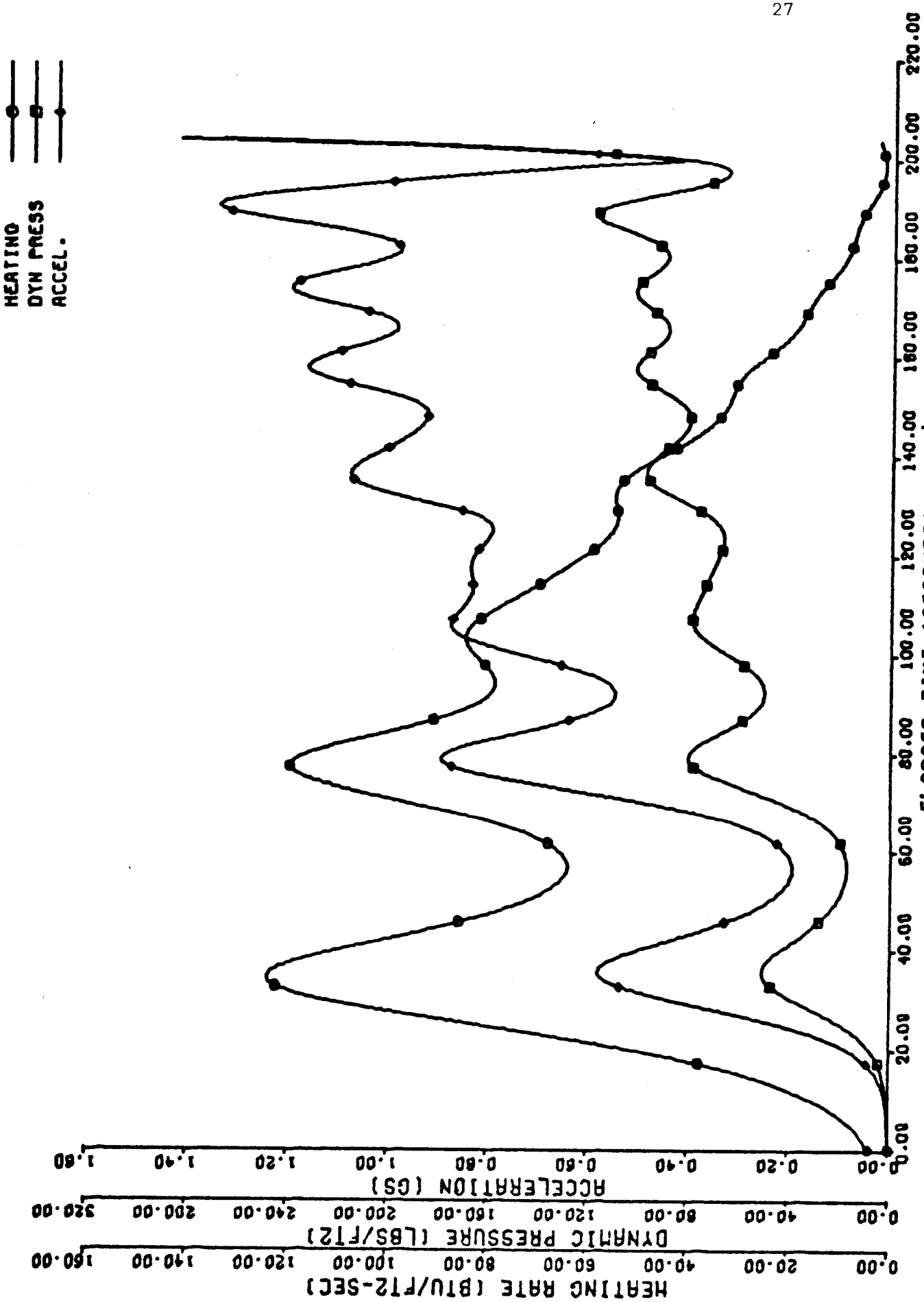

Figure 10. Reference Heating Rate, Dynamic Pressure and Load Factor versus Time

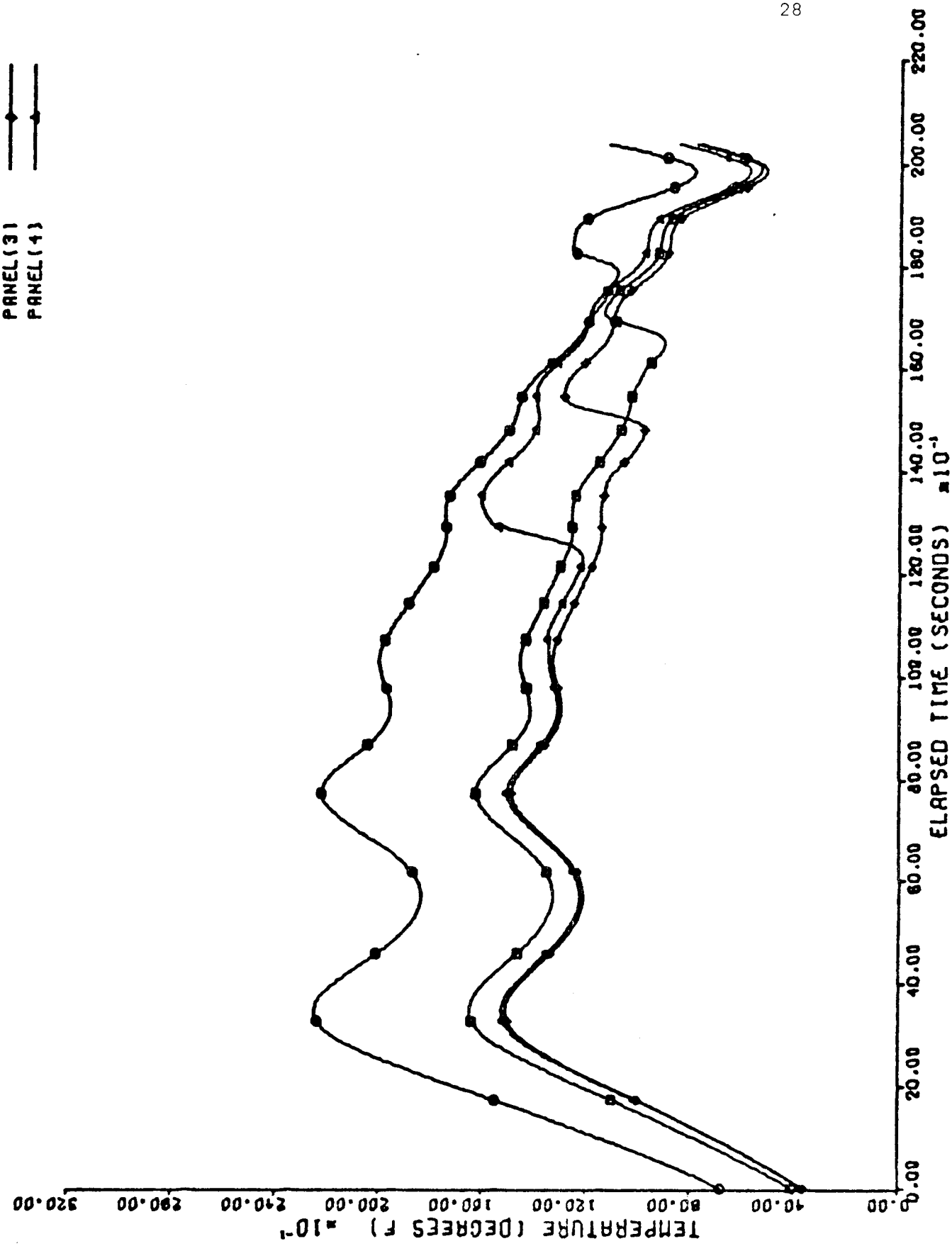

Figure 11. Fuselage Panel Temperatures versus Time

IX. Guidance

A three-dimensional optimum reentry trajectory found in the earlier part of this study was used as the reference trajectory for the guidance studies. The dynamical model of Section III was used and a first-order guidance algorithm was implemented. The first-order algorithm implemented was a closed loop version of the lambda matrix control algorithm[10, 11]. The details of the algorithm are well known and will not be repeated here, since use of algorithm for shuttle reentry guidance produced unsatisfactory performance.

When state errors were introduced, the lambda matrix control guidance scheme produced terminal state errors which were three to ten times larger than the errors experienced when no guidance at all was used. Also, due to the nature of the perturbation equations, first-order control schemes cannot correct state errors in longitude at all. This was felt to be a significant shortcoming.

Typical guidance simulation results are as follows. Starting with an initial state error in altitude of + 1/2 mile at the initial time, the guidance algorithm missed the desired terminal point by over 150 miles while the uncorrected error produced a trajectory which missed the desired terminal point by about 50 miles. Other first-order simulations resulted in even larger terminal state errors.

The programs developed for the guidance study were developed with the idea that the initial choice of guidance algorithm might well be wrong and that the programming should be set up in such a way that the guidance algorithm could be easily changed. The programming for the guidance study was divided into three parts.

The first part (Program A) generates the nominal reference trajectory and stores it on tape. Program A is a reduced version of the trajectory optimization program developed as the primary tool for the reentry optimization study. This program segment will remain the same regardless of the guidance algorithm being tested.

The second part (Program B) contains routines for input of the reference trajectory, routines for the computation of the guidance gains (implementation of the particular guidance algorithm under study), and routines for the output onto tape of the reference trajectory plus the guidance gains information. When changing guidance algorithms, almost all of the required programming changes will be in the gain computation segment of Program B.

The third part (Program C) is very short. The program consists of input routines, a numerical integrator, and a small section of code which produces control changes from pre-calculated gains plus known state errors. Execution time for this program is of the order of 10-15 seconds for simulation of a 1600 second reentry. No state variable error prediction is used. Instead, the nonlinear equations of state are integrated from point to point using the corrected controls (control values obtained by adding guidance-produced control deviations to the nominal control values). After each integration step the new state error is computed and the corrected control values for this point are produced.

It is felt that the philosophy employed in designing the three programs for the study of the guidance problem will greatly facilitate the determination of guidance schemes which will perform adequately for the reentry guidance task. It is likely that an extensive study involving the testing of existent guidance algorithms will be necessary to find an algorithm which will perform adequately for shuttle reentry guidance. It is possible that the development of new optimal or sub-optimal guidance algorithms may be necessary. In any case, the guidance programs developed in this study provide a ready tool for the execution of such studies.

X. Conclusions and Recommendations

The problem of optimal reentry of a shuttle-type vehicle has been considered. In particular, trajectories which minimized the heat input to the underside of the fuselage and

satisfied requirements of downrange, terminal velocity and high crossrange have been computed. The earth has been assumed to be spherical, non-rotating and to possess an inverse square gravitational force field. In addition, the atmosphere has been considered to be at rest with respect to the earth and to vary exponentially with altitude. Control of the vehicle has been affected through variation of the angle of attack and roll angle. The aerodynamic coefficients of lift and drag have been considered to be independent of Mach number and Reynolds number and were obtained from Newtonian flow theory.

The method of perturbation functions (MPF), a second order technique, has been used to generate the trajectories and, although troubled at times by the sensitivity of the trajectories to changes in initial conditions, has proved to be an effective technique for generating families of solutions, once an initial trajectory has been obtained.

The principle areas in which this study warrants extension are (1) improved aerodynamic and atmospheric models, (2) improved methods for generating the corrections to the unknown initial conditions and (3) investigation of the use of multi-shooting or intermediate matching techniques, as opposed to the single-shooting method discussed here, in an effort to reduce sensitivity problems.

REFERENCES

1. McCarthy, John F., "Entry from Lunar and Planetary Missions," Reentry and Planetary Entry Physics and Technology, II/Advanced Concepts, Experiments, Guidance-Control and Technology, W. H. T. Loh, ed., Springer-Verlag, New York 1968, Chap. 11, p. 105.

2. Bryson, A. E. and Y. C. Ho, Applied Optimal Control, Blaisdell, Waltham, Mass., 1969.

3. Williamson, W. E., Jr., "Optimal Three-Dimensional Reentry Trajectories for Apollo-Type Vehicles," Ph.D. Dissertation, University of Texas at Austin, 1970.

4. Zadeh, L. A. and C. A. Desser, Linear System Theory, McGraw-Hill, New York, 1963.

5. Quirein, J. A., "Development of a Subroutine to Compute Heating Rate Factors," TRW IOC 4913, 7-71-147, 20 July, 1971.

6. Fehlberg, E., "Classical Fifth-, Sixth-, Seventh-, and Eighth-Order Runge-Kutta Formulas with Stepsize Control," NASA TR-R287, October 1968.

7. Lastman, G. L. and B. D. Tapley, "Optimization of Nonlinear Systems with Inequality Constraints Explicitly Containing the Control," Int. J. Control, 1970, Vol. 12, No. 3, p. 497-510.

8. Volgenau, E., "Boost Glide and Reentry Guidance and Control," Guidance and Control of Aerospace Vehicles, C. T. Leondes, ed., McGraw-Hill, New York, 1963, Chap. 10, p. 475.

9. Bryson, A. E., W. F. Denham, F. J. Carroll, and K. Mikami, "Determination of Lift or Drag Programs to Minimize Reentry Heating," Journal of Aerospace Sciences, April 1962, p. 420-430.

10. Bryson, A. E., and W. F. Denham, A Steepest-Ascent Method for Solving Optimum Programming Problems, Report BR-1303, The Raytheon Company, August 1961.

11. Fowler, W. T., "First Order Control for Low Thrust Interplanetary Vehicles," Ph.D. Dissertation, The University of Texas, May 1965.

12. Anonymous, Shuttle--The Space Transporter of the 1980's, North American Rockwell, Space Division, 1971.

Appendix A: Constants

This appendix contains all relevant constants used in the reentry problem.

$C_{L_o} = 2.3$

$C_{D_o} = .0786$

$C_{D_L} = 2.09$

$\lambda_c = 1.0 \times 10^{-7}$

$k = 1.4076519 \times 10^{16}$ ft^3/sec^2

$k_c = 17600\ \rho_o^{-0.5}\ V_c^{-3.15}$ BTU/ft^2-sec)

$k_d = 4.2 \times 10^{-5}$ 1/ft

$k_g = \frac{2.5}{(1.5) \cdot 3}$

$k_R = \frac{5.1 \times 10^6}{(2116 \times 5280)^{1.5}}$

$S = 6084$ ft^2

$W = 214{,}861$ lbs

$\rho_o = 2.7 \times 10^{-3}$ slugs/ft^3

$r_e = 3960$ miles

$s_1 = 431$ ft^2

$s_2 = 928$ ft^2

$s_3 = 1306$ ft^2

$s_4 = 1408$ ft^2

$R_{L_1} = 1.94 \times 10^4$ 1/ft

$R_{L_2} = 1.2 \times 10^4$ 1/ft

$R_{L_3} = 7.0 \times 10^3$ 1/ft

$R_{L_4} = 3.5 \times 10^3$ 1/ft

$b_1 = 0.1602$, $c_1 = 0.0781$

$b_2 = 0.0505$, $c_2 = 0.156$

$b_3 = 0.0419$, $c_3 = 0.065$

$b_4 = 0.0451$, $c_4 = 0.039$

$a_1 = -704.9$

$a_2 = 2974.9$

$a_3 = 4952.3667$

$a_4 = 4066.7$

$a_5 = 1646.4$

$a_6 = 263.0667$

$$m = \frac{Wr_e^2}{k} \text{ slugs}$$

$$V_c = \sqrt{\frac{k}{r_e}}$$

$\sigma = 4.761 \times 10^{-13}$ BTU/(sec-ft^2 - (°R)^4)

$\varepsilon_s = 0.8$

Appendix B: Description of Program and Input

The basic flowchart for SHØPDP is shown below.

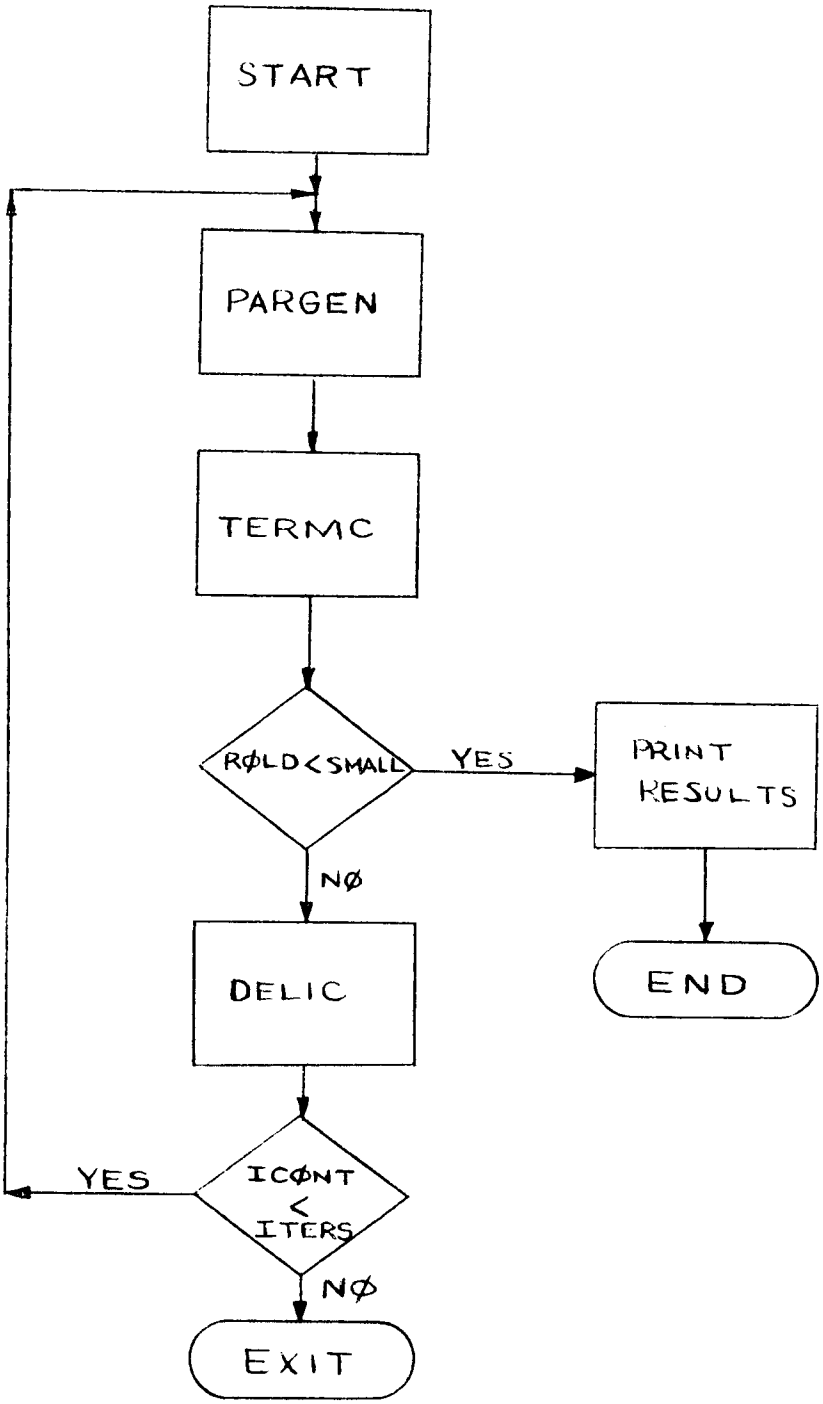

The following is a list accompanied by a brief description of each of the subroutines comprising the program.

SHØPDP -- Main program which contains the basic iteration philosophy of the method.

START --- Called by SHOPDP, sets up all relevant constants and initial guesses for the unknown multipliers and final time.

SETUP --- Called by PARGEN, initializes the matrix DEP which contains the states, multipliers and fundamental matrix.

PARCHE -- Called by SHOPDP, computes the fundamental matrix by integration of the perturbation equations and by numerical differences for comparison.

PARGEN -- Called by PARCHE and by SHOPDP. Computes the fundamental matrix by integration of linear perturbation equations (MPART = 1) or by numerical differences (MPART = 2).

INTGRT -- Called by PARGEN and by CORVEC. Performs integration of equations by RK 7(8) (METH = 1) or by RK 4(5) (METH = 2).

ØUTPT --- Prints states, multipliers and time. Called by RK 7(8) or RK 4(5) according to the print increment specified by IP in call to INTGRT. Converts altitude from miles to feet, longitude to downrange in miles, latitude to crossrange in miles, and velocity from miles per second to feet per second.

DERZ ---- Derivative routine for states and multipliers. Called by RK 7(8) or RK 4(5).

DERZST -- Derivative routine for states, multipliers and linear perturbation equations. Called by RK 7(8) or RK 4(5).

TERMC --- Evaluates terminal dissatisfaction vector and its norm, ROLD. Called by SHOPDP.

DELIC --- Sets up the linear system to be solved for the required changes $\delta\lambda_o$ and δt_f . Called by SHOPDP.

LSSDP --- Called by DELIC. Solves for $\delta\lambda_o$ and δt_f by Gaussian elimination. The matrix input to LSSDP is destroyed.

CØRVEC -- Called by DELIC. Scales the corrections computed in DELIC in a method specified by the parameter KCOR. See listing.

ESTPCT -- Function called by CORVEC which solves for the percent correction corresponding to the minimum of a parabola fit through three successive values of the norm of the terminal dissatisfaction.

DENSIT -- Evaluates density and its first and second derivatives with respect to altitude. Exponential atmosphere. Called by EQMAT.

CUBERT -- Function called by UBOUND which evaluates the 1/3 power of a function.

BNDRYL -- Called by PRFIND and TESTS. Evaluates the boundary layer functions and their derivatives.

REG ----- Function which evaluates the normalized miss distance to the entrance and exit points on a control boundary. Called by TESTS.

UNBØUND -- Computes angle of attack for acceleration constraint. Called by UOPT but is not active in this deck.

KWHICH -- Function called by UOPT which sets a flag which indicates whether the equations of motion are to be evaluated on a constraint boundary or not.

FLAGSE -- Sets all flags for integration and boundaries. Called by PARGEN, SETUP, CORVEC.

PRFIND -- Evaluates performance index and its derivatives. Called by EQMAT.

UØPT ---- Evaluates the optimal control or bounded control and the relevant derivatives of the control. Called by EQMAT.

TESTS --- Performs tests to determine if a constraint boundary is exceeded. Contains iteration philosophy to hit entrance and exit point to boundary. Called by RK 7(8) or RK 4(5).

EQMAT --- Called by DERZ or DERZST. Evaluates derivatives of the states and multipliers and the non zero elements of the matrix of partial derivatives for the linear perturbation equations.

RK 7(8) - Called by INTGRT. Variable step seventh-order Runge-Kutta integrator using Fehlberg coefficients.

RK 4(5) - Called by INGRT. Variable step fourth-order Runge-Kutta integrator using Fehlberg coefficients.

RKCØN --- Called by START. Sets up coefficients for RK 7(8) and RK 4(5).

Description of Input

Data is input to the program through the following namelists.

INTGRT

AERØ

PICØN

IBC

FBC

The following is a description of the variables input through the namelists.

INTGRT:

SMALL --- Stopping condition for iteration. If the norm of the dissatisfaction vector is less than SMALL, the program terminates.

PCTN ---- Specified fraction of correction to be taken, see KCOR.

IPQ ----- Print increment for integration of state, multipliers and linear perturbation equations. If IPQ > 0 stepsize is based only on the state and multipliers. If IPQ < 0 , stepsize is based on all variables.

IPR ----- Print increment when integrating state and multipliers only.

TØL ----- Error tolerance for integration.

KCØR ---- Specifies type of correction scaling procedure. See listing of subroutine DELIC.

CLØSE --- Tolerance to which entrance and exit of control boundaries are satisfied.

KPAR ---- KPAR < 0 Analytic and numerical partials are computed, program terminates.

KPAR > 0 Same as above except program continues iteration.

KPAR = 0 No action, program continues.

DELT ---- Initial integration stepsize, seconds.

MPART --- MPART = 1 Analytic partials are used.

MPART = 2 Numerical partials are used.

METH ---- METH = 1 Integration by RK 7(8).

METH = 2 Integration by RK 4(5).

ITERS --- Maximum number of iterations allowed. If ICOUNT = ITERS, program stops.

SIGDIG -- If the absolute value of relative terminal dissatisfaction of a state is less than SIGDIG the dissatisfaction is weighted according to that element of WTF.

ERPS ---- If the absolute value of a variable is less than ERPS, absolute truncation error is used on that variable in computing an integration stepsize.

DVID ---- Factor which reduces the predicted stepsize to avoid numerous rejection of steps.

KBUG ---- KBUG $\neq$ 0 All namelists are printed.

KBUG = 0 No namelists are printed.

AERØ:

CLZERØ -- Coefficient in Newtonian lift equation.

CDZERØ -- Coefficient in Newtonian drag equation.

CDL ----- Coefficient in Newtonian drag equation.

S ------- Vehicle reference area, ft^2.

WT ------ Vehicle weight, lbs.

AMAX ---- Maximum angle of attack, degrees.

AMIN ---- Minimum angle of attack, degrees.

BMX ----- Maximum roll angle, degrees.

BMN ----- Minimum roll angle, degrees.

PICØN:

A1 ------ Coefficient of performance index.

A2 ------ Weighting factor for penalty function on dynamic pressure.

A3 ------ Weighting factor for penalty function on flight path angle.

A4 ------ Weighting factor for penalty function on reference heating rate.

AP ------ Panel areas, ft^2.

BJ ------ Coefficients of function of angle of attack in heating equation.

CJ ------ Coefficients of function of angle of attack in heating equation.

RL ------ Transition Reynolds number for panels.

TMX ----- Temperature used to specify maximum reference heating rate allowable.

QL ------ Maximum acceleration limit (not active).

CHAPMA -- Chapman heating constant, 17600.

JTEST --- JTEST = 0 Iteration to hit control boundaries is performed.

JTEST ≠ 0 Boundaries are ignored.

NPAN ---- Number of panels.

IBC:

ZI ------ Initial conditions for states and multipliers and final time.

ZI(1) = Altitude, feet.

ZI(2) = Downrange, miles.

ZI(3) = Crossrange, miles.

ZI(4) = Velocity, feet per second.

ZI(5) = Flight path angle, degrees.

ZI(6) = Heading angle, degrees.

ZI(7) thru ZI(12), Multipliers.

ZI(13) = Final time, seconds.

KINPT --- If desired, multipliers and final time can be input in octal. For KINPT = 0 read in the multipliers following Namelist IBC in a 3Ø20 format.

GAM ----- In order to avoid the singularity in flight path angle, integration is terminated if the magnitude of the flight path angle exceeds GAM. The time at which this occurs is taken as a new final time and the program continues.

FBC:

ZFN ----- Terminal conditions for states and multipliers. The units are the same as for ZI in IBC.

KTC ----- A vector which specifies which elements of the ZFN vector are to be satisfied. For example, if KTC consists of 7, 8, 3, 4, 11, 12. Then, the terminal conditions to be satisfied are

$$\lambda_r - \text{ZFN (7)} = 0$$

$$\lambda_\theta - \text{ZFN (8)} = 0$$

$$\phi - \text{ZFN (3)} = 0$$

$$V - \text{ZFN (4)} = 0$$

$$\lambda_\gamma - \text{ZFN (11)} = 0$$

$$\lambda_\psi - \text{ZFN (12)} = 0$$

as well as

$$H(t_f) = 0$$

for free final time.

JTFIX --- JTFIX = 1 Normal Newton-Raphson solution for $\delta\lambda_o$ and δt_f .

JTFIX = 2 Fixed final time.

JTFIX = 3 Selected elements of the KTC vector are satisfied in a least square manner according to LSQ.

LSQ ----- A vector which specifies which of the elements of the KTC vector are to be

satisfied in a least square manner. For example, if LSQ consists of 1, 2, 5, 6, 7 then for those elements specified in KTC above, only terminal conditions on the multipliers λ_r, λ_θ, λ_γ, λ_ψ and $H(t_f)$ are treated.

NTC ----- Number of terminal conditions specified for the least square solution. In the example above, NTC = 5 .

WTF ----- Weighting values to be applied to a terminal dissatisfaction to reduce its importance in the solution for the changes $\delta\lambda_o$ and δt_f .

NØJØY --- Print flag.

|NØJØY| = 1 Angle of attack and roll angle are printed on each integrated step.

NØJØY < 0 Every iterate to enter or exit a control boundary is printed.